Application of Direct Assimilation of ATOVS Microwave Radiances to Typhoon Track Prediction

ZHANG Hua*[1,2] (张 华), XUE Jishan[2] (薛纪善), ZHU Guofu[2] (朱国富), ZHUANG Shiyu[2] (庄世宇), WU Xuebao[3] (吴雪宝), and ZHANG Fengying[3] (张风英)

[1] *Atmospheric Science Department, Lanzhou University, Lanzhou* 730000

[2] *Chinese Academy of Meteorological Sciences, China Meteorological Adminstration, Beijing* 100081

[3] *National Satellite Meteorological Center, China Meteorological Adminstration, Beijing* 100081

(Received 30 July 2003; revised 8 December 2003)

ABSTRACT

In order to solve the difficult problem of typhoon track prediction due to the sparsity of conventional data over the tropical ocean, in this paper, the No. 0205 typhoon Rammasun of 4–6 July 2002 is studied and an experiment of the typhoon track prediction is made with the direct use of the Advanced TIROS-N Operational Vertical Sounder (ATOVS) microwave radiance data in three-dimensional variational data assimilation. The prediction result shows that the experiment with the ATOVS microwave radiance data can not only successfully predict the observed fact that typhoon Rammasun moves northward and turns right, but can also simulate the action of the fast movement of the typhoon, which cannot be simulated with only conventional radiosonde data. The skill of the typhoon track prediction with the ATOVS microwave radiance data is much better than that without the ATOVS data. The typhoon track prediction of the former scheme is consistent in time and in location with the observation. The direct assimilation of ATOVS microwave radiance data is an available way to solve the problem of the sparse observation data over the tropical ocean, and has great potential in being applied to typhoon track prediction.

Key words: radiance, direct assimilation, typhoon track prediction

1. Introduction

For a long time, the lack of sufficient observational data has been one of the major obstacles to understanding typhoon movement in the Northwest Pacific further and to predicting the typhoon accurately. Typhoon or tropical cyclone (TC) track prediction, especially abnormal typhoon track prediction, is one of the three unsolved difficult problems related to typhoon research in the world today. In many earlier research works (Neumann, 1979; Sanders et al., 1980; Keenan, 1982; Holland, 1984), a typhoon was considered as a point vortex moving in uniform airflow without interaction, and the concept of steering flow was proposed. In reality, typhoon track prediction with this kind of model often produces large errors. With the development of atmospheric science theory and progress in sounding techniques, scientists gradually recognized that typhoon movement is influenced by various complex factors. Chen and Luo (1995a) showed that the asymmetric structure of the inner core of a tropical cyclone could influence its movements apparently. Chen et al. (1997) further showed that not only the dynamical asymmetric structure but also the thermodynamical asymmetric structure of a tropical cyclone could influence its movements. Furthermore, the movements can be influenced by environmental systems of different scales (Chen and Luo 1995b; Zhu 1996; Meng et al., 2002). Owing to the lack of key observation data over the vast tropical ocean and the limitation of data analysis techniques, it is difficult to directly obtain the initial fields that are needed in the forecast models to reflect the characteristics of the actual typhoon structure. The results of Qu and Heming (2002) showed that dropsonde data could improve TC track forecasts. At present, an artificial typhoon is constructed (bogus data) as an initial field in the model. Several operational centers, such as the Japan Meteorological

*E-mail: zhangh@cma.gov.cn

Administration, the National Meteorological Center of China, the Guangzhou Tropical Ocean Institute, the Shanghai Typhoon Institute, etc., use this technique. Thus the typhoon track predictions are improved.

The appearance of the meteorological satellite was an epoch-making event in atmospheric sounding techniques. The use of meteorological satellites can obtain a larger coverage area, even distribution, and higher spatial resolution for atmospheric information, and it can solve the problem of the lack of conventional data in the depopulated zones of ocean, plateau, and desert, which cannot be solved by conventional observation systems. A preliminary study was carried out on the employment of satellite cloud-derived wind which showed some positive impacts on TC track forecasts (Zhang and Wang, 1999); the study showed that cloud-derived wind data may improve the wind analysis field and consequently improve TC track prediction. Another study showed that TC track and rainfall prediction could be apparently improved with the use of a modified diabatic heating scheme based on the distribution of satellite brightness temperature (Zhou and Zhu, 1999).

In particular, the NOAA (the National Oceanic and Atmospheric Administration) polar-orbiting meteorological satellite-borne Advanced Microwave Sounding Unit (AMSU) can not only detect vertical profiles of atmospheric temperature and humidity, but it also has the unique ability to penetrate through heavy cloud layers, except for precipitation clouds, and it can detect the inner structure of typhoons. The difficulty is that the meteorological satellite does not directly sound the atmospheric temperature and humidity but it sounds the thermal radiances within many frequency bands, which radiate into space. There is some complicated nonlinear relationship between thermal radiances and atmospheric variables, thus the conventional analysis method based on spatial interpolation cannot be used. In numerical weather prediction, there are two main ways to apply satellite radiance data. First, satellite sounding radiance data are converted to the atmospheric variables of temperature and humidity using the physical retrieval method, and then the retrieved data are assimilated in the same way as conventional observation data. This method has two problems: (1) the ill-posedness of the retrieval calculation; (2) the inconsistency between the first-guess values of the retrieved data and the initial field of the numerical weather prediction model in the numerical prediction operational centers. The second main way to use satellite radiance data is through direct assimilation, based on the three-dimensional variational (3DVAR) assimilation technique (Courtier et al., 1994; Courtier et al., 1996; Courtier, 1997; Lorenc, 1997). The fundamental idea is that the simulated radiances are calculated using analysis variables through the atmospheric transfer equation, and the differences between the simulated radiances and the observed radiances are also calculated. Adding certain constraint conditions, constructing a cost function, and using the optimum method, the analysis variables are then obtained in the minimizing process (Eyre et al., 1993; Andersson et al., 1994; Rabier et al., 2000). The method can not only analyze satellite radiance data that have a complicated nonlinear relationship with the model variables, but can also effectively analyze different kinds of observed data that have different error characteristics, and can carry out the integration of the retrieval and the analysis in one step. Moreover, this method can effectively overcome the ill-posedness difficulty in the retrieval problem with the forward method to avoid the complexity of the retrieval problem.

Zhang (2003) used ATOVS microwave data in a 3DVAR assimilation analysis to study the typhoon structure over the Northwest Pacific and the change of the typhoon structure in different periods. The study shows that ATOVS microwave assimilation data can correctly describe the characteristics and changes of the typhoon 3D structure over the Northwest Pacific, which cannot be obtained using conventional observed data. Based on this work, we further study, the impact of ATOVS microwave assimilation data on typhoon track prediction. In this paper, the introduction is given in section 1; in section 2, the characteristics of the AMSU microwave data and its assimilation analysis method are introduced; the numerical prediction model is simply introduced in section 3; the numerical experiments and analysis are carried out in section 4; and conclusions are stated in section 5.

2. The direct assimilation analysis method of ATOVS radiance data

2.1 *3DVAR assimilation method*

The fundamental idea of the 3DVAR assimilation method is to find the closest solution between the effective observation and background field (the first guess) in the given periods under the meaning of the least square method by adjusting the first guess. The function (also called the cost function) is generally defined as

$$J = \frac{1}{2}(\boldsymbol{x}-\boldsymbol{x}_\mathrm{b})^\mathrm{T}\boldsymbol{B}^{-1}(\boldsymbol{x}-\boldsymbol{x}_\mathrm{b}) + \frac{1}{2}(\boldsymbol{y}-\boldsymbol{y}_\mathrm{o})^\mathrm{T}\boldsymbol{O}^{-1}(\boldsymbol{y}-\boldsymbol{y}_\mathrm{o}) \quad (1)$$

where $\boldsymbol{x}$ is the analysis vector (on model grid points), $\boldsymbol{x}_\mathrm{b}$ is the background vector (on model grid points)

with dimension N (the number of model grid points), $\boldsymbol{y}_{\rm o}$ is the observational vector (on observation locations) with dimension M (the number of observations), y is the observation vector derived from $\boldsymbol{x}, B^{-1}$ is the inverse of the covariance matrix of the background error with the order of $N \times N, \boldsymbol{O}^{-1}$ is the inverse of covariance matrix of the observational error with the order of $M \times M$.

$\boldsymbol{y}$ is given by $\boldsymbol{y} = H(\boldsymbol{x}), H$ is the observation operator, which represents the mapping from the model space to the observation space.

In principle, the analysis vector $\boldsymbol{x}$ which minimizes the cost function J can be found using a descent algorithm, using some software to calculate J and its gradient $\nabla_{\boldsymbol{x}} J$. For the practical solution of this problem, two transformations are made: the transformation to increments and the transformation to a preconditioned analysis variable.

2.1.1 *Incremental approach*

According to Courtier et al. (1994), the incremental approach is used to solve the computational expense problem in the evaluation of the cost function in the minimizing process.

Expand observation operator $H(\boldsymbol{x})$ at $\boldsymbol{x}_{\rm b}$ as a Taylor series, and truncate to the first two terms:

$$H(\boldsymbol{x}) = H(\boldsymbol{x}_{\rm b} + \delta\boldsymbol{x}) \approx H(\boldsymbol{x}_{\rm b}) + H'\delta\boldsymbol{x} \,, \qquad (2)$$

where .

$$H' = \frac{\partial H}{\partial x} \,, \quad \delta\boldsymbol{x} = \boldsymbol{x} - \boldsymbol{x}_{\rm b} \,.$$

Let

$$\boldsymbol{d} = H(\boldsymbol{x}_{\rm b}) - \boldsymbol{y}_{\rm o} \,, \qquad (3)$$

J can be expressed as

$$J = \frac{1}{2}\delta\boldsymbol{x}^{\rm T}\boldsymbol{B}^{-1}\delta\boldsymbol{x} + \frac{1}{2}(H'\delta\boldsymbol{x}+\boldsymbol{d})^{\rm T}\boldsymbol{O}^{-1}(H'\delta\boldsymbol{x}+\boldsymbol{d}) \,, \qquad (4)$$

and its gradient as

$$\nabla_{\delta\boldsymbol{x}} J = \boldsymbol{B}^{-1}\delta\boldsymbol{x} + H'^{\rm T}\boldsymbol{O}^{-1}(H'\delta\boldsymbol{x}+\boldsymbol{d}) \qquad (5)$$

2.1.2 *Preconditioning*

It is well known that numerical methods for matrix inversion are very sensitive to the conditioning of the matrix to invert. Mathematically, the conditioning number is defined as the ratio of the largest eigenvalue to the smallest if the matrix is semi-positive definite. In practice, a large conditioning number tends to slow down or stop the convergence of the iterative process. On the other hand, a matrix with a conditioning number close to 1 tends to speed up the convergence of the iterative process.

For a practical solution, the analysis variables are designed to improve the conditioning of the Hessian matrix in the minimization process. The Hessian is a matrix of second-order partial derivatives with respect to the analysis variables.

$$\nabla^2_{\delta\boldsymbol{x}} J = \boldsymbol{B}^{-1} + H^{\rm T}\boldsymbol{O}^{-1}H \,. \qquad (6)$$

The observation operator H in the second term of (6) is dependant on the observing system. It is hard to analyze the exact conditioning number in a general way. So one should concentrate on the first term of (6), which depends on the background error covariance matrix $\boldsymbol{B}^{-1}$ only. It has been observed that errors in background term usually come from balanced and smooth modes, which corresponds to small eigenvalues of $\boldsymbol{B}^{-1}$, while there exist some unbalanced or rough model, which corresponds to large eigenvalues of $\boldsymbol{B}^{-1}$. This large range of eigenvalues means that $\boldsymbol{B}^{-1}$ is ill-conditiond. To avoid the computational difficulty and to improve the convergence, a variable transformation is used to precondition the cost function (Lorenc, 1997). The new analysis variable $\boldsymbol{w}$ is defined as

$$\delta\boldsymbol{x} = \sqrt{\boldsymbol{B}}\boldsymbol{w} \qquad (7)$$

Substituting (7) into (4) and (5), the cost function and its gradient after transformation can be obtained

$$J = \frac{1}{2}\boldsymbol{w}^{\rm T}\boldsymbol{w} + \frac{1}{2}(H'\sqrt{\boldsymbol{B}}\boldsymbol{w}+\boldsymbol{d})^{\rm T}\boldsymbol{O}^{-1}(H'\sqrt{\boldsymbol{B}}\boldsymbol{w}+\boldsymbol{d}) \,, \qquad (8)$$

$$\nabla_w J = \boldsymbol{w} + \sqrt{\boldsymbol{B}}^{\rm T}H'^{\rm T}\boldsymbol{O}^{-1}(H'\sqrt{\boldsymbol{B}}\boldsymbol{w}+\boldsymbol{d}) \,, \qquad (9)$$

and the Hessian as

$$\nabla^2_w J = \boldsymbol{I} + \sqrt{\boldsymbol{B}}^{\rm T}H^{\rm T}\boldsymbol{O}^{-1}H\sqrt{\boldsymbol{B}} \,, \qquad (10)$$

where $\boldsymbol{I}$ is the identity matrix. This new Hessian matrix (10) is expected to be much better conditioned than the old one (6). Formulae (8) and (9) are the cost function and its gradient in our scheme. In the case of ATOVS radiances, H mainly represents a radiative transfer model.

2.1.3 *The fast radiative transfer model RTTOV*

RTTOV (Radiative Transfer for TIROS-N Operational Vertical Sounder) is a fast radiative transfer model which has been under development at ECMWF since 1990 (Saunders et al., 1999). It computes top-of-atmosphere radiances and equivalent blackbody brightness temperatures for satellite infrared and microwave radiometers given an input atmospheric profile of temperature, water vapor and optionally ozone and cloud liquid water. It supports many different satellite radiance observations such as the NOAA (National Oceanic and Atmospheric Administration) series of polar-orbiting satellites, the GOES (The Geostationary Operational Environmental Satellite) series of stationary satellites, etc.

The model uses an approximate form of the atmo-

spheric radiative transfer (RT) equation.

$$L(\nu,\theta) = \tau(\nu,\theta,p_{\rm s})A(\nu,T_{\rm s}) - \int_0^{p_{\rm s}} A[\nu,T(p)]\frac{\partial\tau(\nu,\theta,p)}{\partial p}dp\,, \qquad (11)$$

where $L(\nu,\theta)$ is upwelling radiance on the top of the atmosphere at a frequency ν and viewing angle θ from zenith at the surface. the first item of equation (11) is the radiance from the surface (emitted and reflected assuming specular reflection) and the second item is the radiance emitted by the atmosphere $A(\nu,T)$ is the Planck function for a scene temperature, $\tau(\nu,\theta,p)$ is the surface to space transmittance, $\tau(\nu,\theta,p)$ is the layer to space transmittance. T is the layer mean temperature and $T_{\rm s}$, the surface temperature. p is the pressure of layer and $p_{\rm s}$, the surface pressure.

For a practical solution, the observation operator H consists of four parts

$$H = H_{\rm S}H_{\rm RT}H_{\rm V}H_{\rm H} \qquad (12)$$

where $H_{\rm H}$ is the horizontal interpolation operator, i.e., the gridpoint data of the background field (prediction model) are interpolated using a bi-linear interpolation onto the view field on which the observed brightness temperature data are located; $H_{\rm V}$ is the vertical interpolation operator, i.e., through the horizontal interpolation, the data on the levels of the prediction model are interpolated vertically to the levels of the radiance transfer model RTTOV (Saunders et al., 1999), a natural logarithm bi-linear interpolation is adopted within the levels of the prediction model (1000 hPa–10 hPa), and an extrapolation is adopted above the top level of the prediction model and below its bottom level; $H_{\rm RT}$ is the radiance transfer forward operator RTTOV; and $H_{\rm S}$ is the channel selection operator. $(\ )'$ is the tangential linear operator and $(\ )^{\rm T}$ is the corresponding adjointing operator.

2.2 *Quality control*

Many factors can cause large errors in satellite observations, such as the weather conditions (clear, cloudy, or overcast), the ground conditions (sea surface, land, sea ice, etc.), the geographical location (as in middle-latitudes or the Tropics), observational geometrical conditions (sub-satellite point or an edge measure), the response characteristics and accuracy in the process of the sensor moving in the orbit, the error of the forward model and the error of the background field, and so on. In order to guarantee consistency between neighboring data and quality of the analysis result, quality control procedures must be done first. In this paper, they are a check for extreme values, a check for departures between the background field of the simulated observation value and the actual observation value, and cloud detection.

2.2.1 *Extreme value check*

The radiance brihness temperature data in the range 150°C–350°C, so observed data outside of the interval are rejected.

2.2.2 *A check for departures between the background field of the simulated observation value and the actual observation value*

Using the threshold check, the radiance brightness temperature data that cannot satisfy the following inequality

$$|\boldsymbol{y}_{{\rm b}i} - \boldsymbol{y}_{0i}| \leqslant k\sigma_0 \qquad (13)$$

are excluded, where $\boldsymbol{y}_{{\rm b}i}$ and y_{0i} are the background field of the simulated observation value and the actual observation value in channel i, respectively; σ_0 is the covariance of radiance brightness temperature data; k is a parameter, set as $k = 6$ according to experimental tests.

2.2.3 *Cloud detection*

Despite the ability of AMSU to penetrate the cloud layer to detect atmospheric temperature and humidity, the water droplets and ice crystals in precipitation cloud are larger than the radiance wavelength, so the resulting scatter can weaken the signal below the cloud layer. This influences the detection, thus the presence of precipitation cloud must be checked. According to the precipitation probability (unit: %) of the ATOVS 1D dataset, we use

$$P = \frac{1}{1+e^{-f}}\,, \qquad (14)$$

$$f = 10.5 + 0.184T_{\rm B1} - 0.221T_{\rm B15} \qquad (15)$$

where $T_{\rm B1}$ and $T_{\rm B15}$ are the observation brightness temperature in channel 1 and channel 15, respectively. When

$$P \geqslant 70$$

the radiance brightness temperature must be rejected.

2.2.4 *Channel selection*

The channel selection is decided according to the peak energy contribution level of the sounder channel and the influence of the sounding objective on the retrieval results of temperature and water vapor. In order to avoid the negative influence of surface albedo on the retrieval results of temperature and water vapor, channels 1–4 of the microwave sounder AMUS-A and channels 1–2 of AMUS-B are excluded. Channels 12–15 of the microwave sounder AMUS-A are excluded in order to avoid the error caused by the interpolation method above the model's top level that might influence the retrieval results of temperature and water vapor.

2.3 *Data*

The observation data used in the experiments consist of the ATOVS microwave radiance brightness tem-

Table 1. Experiment schemes.

Scheme	Radiosonde data	ATOVS data	Analysis scheme	Prediction model	Model boundary conditions
1	Yes	No	3DVAR assimilation	WRF	T213 model prediction fields (every 3 hours)
2	Yes	Yes	As above	As above	As above

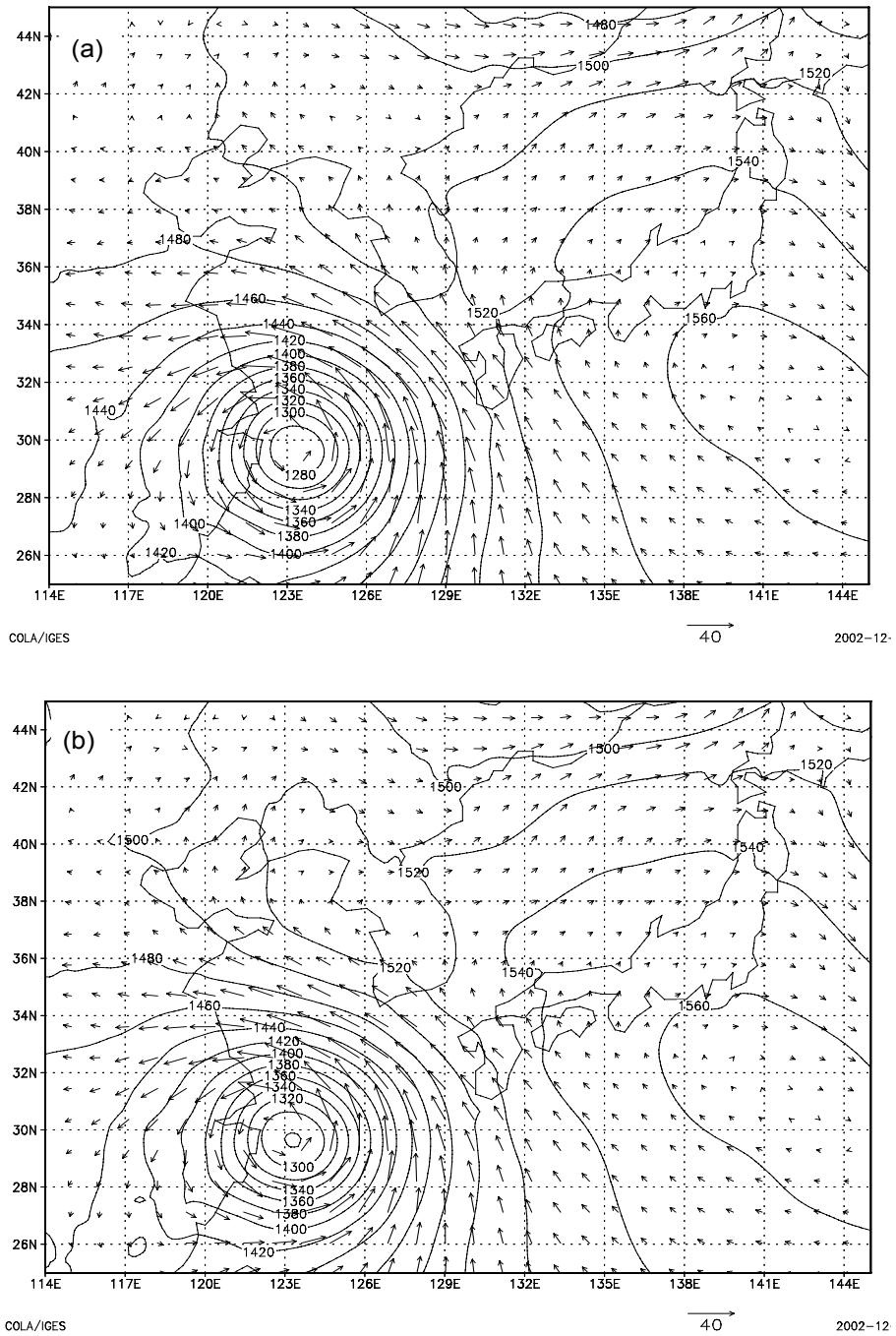

Fig. 1. The initial geopotential height and streamline charts of (a) Experiment 1, and (b) Experiment 2 at 850 hPa at 1500 UTC 4 July 2002 (The contours represent geopotential height with an interval of 20 m, and the arrows represent wind).

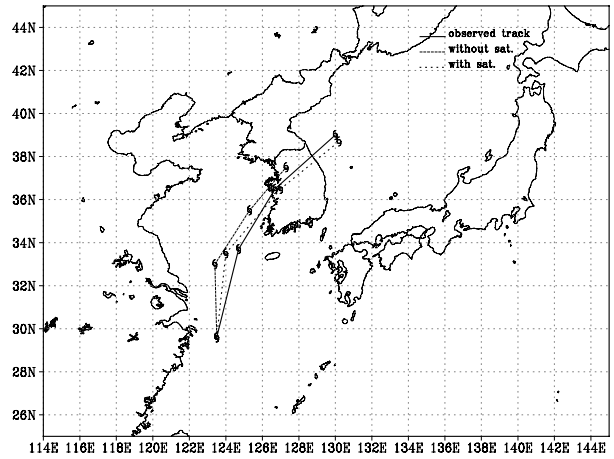

Fig. 2. The typhoon track prediction chart, where the heavy solid line is the observed typhoon track, the dashed line represents Expt.1 (conventional data only) 1 and the dotted line represents Expt. 2 (conventional and satellite data).

perature data of the polar-orbiting satellite NOAA-16 and the conventional radiosonde observation data. The background fields are the prediction fields of the global spectral model T213.

3. Introduction of the numerical prediction model

The Weather Research and Forecast (WRF) model is adopted as the experimental numerical prediction-model. This model is a new generation mesoscale numerical prediction model developed by the National Center for Atmospheric Research (NCAR), NOAA, the Center for Analysis and Prediction of Storms (CAPS) at the University of Oklahoma, and other institutions and universities. WRF is the model for research and operational numerical weather prediction, and will replace the present mesoscale and regional models, such as the Pennsylvania State University (PSU)/NCAR Mesoscale Model (MM5), the Eta model at the National Centers for Environmental Prediction (NCEP), and the Rapid Update Cycle (RUC) system of the Forecast System Laboratory (FSL), etc. In the WRF model, the equations of the perfect, compressible, nonhydrostatic flux form are adopted, the vertical coordinate is the orography-following height coordinate, the horizontal coordinate is the C-type rectangular grid, and the Euler explicit time-split integral scheme is adopted. Considering the more actual orography and underlying surface classification data, the relaxation boundary conditions are used in the lateral boundary. The Betts-Miller-Janjic scheme is used as the cumulus convective parameterization method. The Rapid Radiative Transfer Model (RRTM) scheme is used as the atmospheric longwave radiance parameterization. The Dudhia simplified scheme is used as the solar shortwave radiance parameterization method. The MM5 five-layer soil temperature model is used as the land surface process. The WRF scheme is used in the planetary boundary layer. The model horizontal grid is 150×130. There are 35 vertical layers. The horizontal grid length is 30 km and the time step is 120 seconds.

4. Numerical experiments

4.1 *Case introduction*

The No. 0205 typhoon, Rammasun, over the Northwest Pacific during 4–6 July 2002 is selected to study the typhoon track. At 1500 UTC 4 July, typhoon Rammasun was located at 29.6°N, 123.5°E, then it moved northward. At 0600 UTC 5 July, it began to move northeastward. At 1800 UTC, it moved rapidly across the Korean Peninsula. At 1200 UTC 6 July, typhoon Rammasun arrived at the east side of the Korean Peninsula, with its center located at 38.0°N, 129°E. The action of this typhoon movement consists of turning motion and fast movement. This typhoon is a good case to study the typhoon track using the satellite data.

4.2 *Experiment scheme*

In order to investigate the impact of ATOVS microwave radiance brightness temperature data on the typhoon track prediction, two experiments are carried out. In the first experiment, only the conventional radiosonde data are adopted as the observation data, and the results after the assimilation are accepted as the initial fields of the WRF model for the 45-hour prediction. In the second experiment, the ATOVS microwave radiance brightness temperature data are added into the set of observation data, and other factors are the same as in the first experiment (Table 1).

4.3 *Analysis of experiment results*

Figures 1a and 1b are the 850-hPa geopotential streamline fields of Expt. 1 and Expt. 2, respectively, at the initial time (1500 UTC 4 July). The domain shown in the figures is parts of the actual computational area, i.e., 25°–45°N, 114°–145°E. As shown in the figures, the initial fields of Expt. 1 and Expt. 2 are nearly the same except for the center area of the typhoon; the circulation situation is high in the east and low in the west. The typhoon is located in the southeast seaside of China, and its center is located at 29.6°N, 123°E. The subtropical high is to the east of the typhoon.

Figure 2 is both experiment results of the typhoon track prediction, where the heavy solid line is the observaed track, the dashed line represents Expt. 1, and the dotted line represents Expt. 2. Expt. 1 (with the conventional observation) shows that the typhoon moves northward first, and at hour 21 of the prediction (i.e., 1200 UTC 5 July), the typhoon center is located at 33.0°N, 123.4°E; in comparison with the actual figure (the analysis field of the global spectral model T213 at the same time), the movement of the typhoon is somewhat slow, and it continues to move northward rather than northeastward, and the error of the track prediction is 140 km. At hour 33 of the prediction, the typhoon moves northeastward and close to the Korean Peninsula, with its center located at 35.5°N, 125.3°E. At this time, the center of the typhoon is still lagging the actual position. The error of the track prediction is increased to 160 km. At hour 45 of the prediction, the typhoon continues to move northeastward, and lands at the Korean Peninsula. In comparison with the actual field, Expt. 1 cannot predict the rapid movement of the typhoon across the Korean Peninsula, and the error of the typhoon track prediction is increased to more than 280 km.

The prediction result with the satellite observation data (Expt. 2) shows that the typhoon begins to move northward, the same as Expt. 1 at first. At hour 21 of the prediction, the typhoon center is located at 33.5°N, 124.0°E, which is nearer to the actual field; the northeastward turning of the typhoon after 0600 UTC 5 July is followed (not shown in the figure), and the error of the typhoon track prediction is about 70 km. At hour 33 of the prediction, the typhoon continues to move northeastward, begins to land at the Korean Peninsula, the typhoon center is consistent with the actual one, and the error of the typhoon track prediction is less than 30 km. At hour 45 of the prediction, the simulated typhoon Rammasun moves quickly across the Korean Peninsula, with its center located at 38.7°N, 130.2°E, which is very close to the actual one, and the error of the typhoon track prediction is less than 40 km.

Comparing Expt. 1 with Expt. 2, it can be seen that the directions of the typhoon movement are nearly the same; the process of the typhoon, which moves northward and then turns northeastward can be simulated correctly. Expertment 2, in which the satellite data are added, is somewhat better. But the typhoon displacement speeds of Expt. 1 and Expt. 2 are quite different. The displacement speed of Expt. 1 (in which only the conventional observation data are used) is apparently slow, and the process in which the typhoon passes rapidly over the Korean Peninsula cannot be simulated, and the error of the typhoon track prediction increases with the prediction time. Experiment 2, on the other hand, can not only simulate the typhoon's northward displacement and turning, but can also simulate the rapicl displacement. In Expt. 2, the simulated typhoon is close to the actual observation results in time and in location.

5. Conclusions and discussions

In order to use the ATOVS microwave radiances, to inspect the impact of this kind of data on typhoon track prediction, and to solve the difficult problem of typhoon track prediction due to the lack of conventional observation data over the tropical oceans, the authors use the latest 3DVAR assimilation technique to directly assimilate the ATOVS microwave radiance data, and use them as the initial fields of the prediction model to predict the typhoon track. The No. 0205 typhoon, Rammasun, during 4–6 July 2002 is used as the case study to analyze the impact experiment. The following conclusions are obtained:

(l) The assimilation experimental schemes of different data have a great impact upon the prediction of the typhoon track. Experiment 2 in which the ATOVS microwave radiance data are added can not only correctly predict the tendency of the northward movement and turning of typhoon Rammasun, but can also simulate the rapid displacement of the typhoon which cannot be simulated by using conventional radiosonde data only (Expt. 1). In comparing the prediction result of the experimental scheme with the conventional radiosonde data, the experimental scheme with the ATOVS microwave radiance data apparently improves the track prediction of typhoon Rammasun; the simulated typhoon track using this scheme is consistent with the actual observation result in time and in location.

(2) The ATOVS microwave assimilation data may correctly describe the 3D structure characteristics of a typhoon in the Northwest Pacific and its change characteristics, which cannot be described by conventional observation data (Zhang, 2003). The successful simulation of the sudden acceleration of typhoon Rammasun in Expt. 2 means that the typhoon structure has a great impact upon the variance of typhoon displacement speed.

(3) Both experiments can correctly simulate the displacement direction of the typhoon, which means that the steering flow is still important in the typhoon movement.

(4) In order to overcome the lack of the conventional observation data over the vast tropical ocean, many operational prediction centers widely use the "bogus" technique at the present, which is used to substantially construct a "real typhoon". The successful

typhoon track prediction of Expt. 2 indicates that the direct assimilation of the ATOVS microwave radiance data may improve the "bogus" technique and finally replace it.

With the rapid development of atmospheric science theory and remote sensing sounding techniques, the era of relying mainly on conventional observation data is gone, and the era of relying mainly on unconventional satellite observations is coming. The ATOVS microwave sounding system borne on the NOAA polar-orbiting meteorological satellites not only has the characteristics of a wide coverage area and high sounding accuracy, but also has the ability to penetrate through heavy clouds to detect the vertical structure of the atmospheric temperature and humidity. The results of this experiment and former observation experiments (Zhang, 2003) show that the ATOVS microwave radiance data and their assimilation technique are an effective way to solve the problem of the lack of conventional observation data over the tropical ocean, and has great potential and brilliant prospects in typhoon track prediction.

Acknowledgments. The support of the National Key Scientific Program (Contract 2001BA607B) is gratefully acknowledged. Acknowledgment is also given to Mr. Zhao Gang, Ms. Wan Feng, and Mr. Tao Shiwei of the National Meteorological Center, for offering parts of the data.

REFERENCES

Andersson, E., J. Pailleux, J.-N. Thepaut, J. R. Eyre, A. P. McNally, G. A. Kelly, and P. Courtier, 1994: Use of cloud-clear radiances in three/four- dimensional variational data assimilation. *Quart. J. Roy. Meteor. Soc.* **120**, 627–653.

Chen Lianshou, and Luo Zhexian, 1995a: Some relations between asymmetric structure and motion of typhoons. *Acta Meteorologica Sinica,* **9**(4), 412–419.

Chen Lianshou, and Luo Zhexian, 1995b: Effect of the interaction of different-scale vortices on the structure and motion of typhoon. *Adv. Atmos. Sci.*, **12**(2), 207–214.

Chen Lianshou, Xu Xiangde, Xie Yiyang, and Li Wenhong, 1997: The effect of tropical cyclone asymmetric thermodynamic structure on its unusual motion. *Scientia Atmospherica Sinica*, **21**(1), 83–90. (in Chinese)

Courtier, P., 1997: Variational methods. *J. Meteor. Soc. Japan*, **75**(1B), 211–218.

Courtier, P., J.-N. Thepaut, and A. Hollingsworth, 1994: A strategy for operational implementation of 4D-Var, using an incremental approach. *Quart. J. Roy. Meteor. Soc.*, **120**, 1367–1388.

Courtier, P., and coauthors, 1996: The ECMWF implementation of three-dimensional variational assimilation (3D-Var). I: Formulation. *Quart. J. Roy. Meteor. Soc.*, **124**, 1783–1807.

Eyre, J. R., G. A. Kelly, A. P. McNally, E. Andersson, and A. Persson, 1993: Assimilation of TOVS radiance information through one-dimensional variational analysis. *Quart. J. Roy. Meteor. Soc.*, **119**, 1427–1463.

Holland, G. J., 1984: Tropical cyclone motion: A comparison of theory and observation. *J. Atmos. Sci.,* **41**, 68–75.

Lorenc, A. C., 1997: Development of an operational variational assimilation scheme. *J. Meteor. Soc. Japan*, **75**(1B), 339–346.

Meng Zhiyong, Chen Lianshou, and Xu Xiangde, 2002: Recent progress on tropical cyclone research in China. *Adv. Atmos. Sci.*, **19**, 103–110.

Keenan, T. D., 1982: A diagnostic study of tropical cyclone forecasting in Australia. *Aust. Meteor. Mag.*, **30**, 69–80.

Neumann, C. J., 1979: On the use of deep-layer-mean geopotential height fields in statistical prediction of tropical cyclone motion. *6th Conference on Hurricanes and Tropical Meteorology*, Amer. Meteor. Soc., Boston, 32–38.

Qu Xiaobo, and Julian Heming, 2002: The impact of dropsonde data on forecasts of hurricane Debby by the Meteorological Office Unified Model. *Adv. Atmos. Sci.*, **19**(6), 1029–1044.

Rabier, F., J. Jarvinen, E. Klinker, J. F. Mahfouf, and A. Simmons, 2000: The ECMWF implementation of four-dimensional variational assimilation. I: Experimental results with simplified physics. *Quart. J. Roy. Meteor. Soc.*, **126**, 1143–1170.

Sanders, F., A. L. Adams, N. J. B. Gordon, and W. D. Jensen, 1980: Further development of a barotropic operational model for predicting paths of tropical storms. *Mon. Wea. Rev.*, **108**, 642–654.

Saunders, R., M. Matricardi, and P. Brunel, 1999: A fast radiative transfer model for assimilation of satellite radiance observations–RTTOV-5. ECMWF Tech. Memo., 282pp.

Zhang Hua, 2003: Chapter 5, the application of the ATOVS radiance microwave data (I) —The satellite observation of the typhoon structure in Northwest Pacific, the direct assimilation method and application research of the ATOVS radiance data. Ph. D. dissertation, Lanzhou University, 62–86. (in Chinese)

Zhang Shoufeng, and Wang Shiwen, 1999: Numerical experiments of the prediction of typhoon tracks by using satellite cloud-derived wind. *Journal of Tropical Meteorology*, **15**(4), 347–355. (in Chinese)

Zhou Xiaqiong, and Zhu Yongti, 1999: Numerical study on the effect of asymmetric diabatic heating on tropical cyclone motion. *Quarterly Journal of Applied Meteorology*, **10**(3), 284–292. (in Chinese)

Zhu Yongti, 1996: Numerical study of the influence of the large-scale basic flow speed variance on the tropical cyclone movement. *Typhoon Experiment and Theoretical Research II,* China Meteorological Press, Beijing, 35–41. (in Chinese)